Mie scattering enhanced near-infrared light response of thin-film silicon solar cells

S. Nunomura, A. Minowa, H. Sai, and M. Kondo

Citation: Applied Physics Letters **97**, 063507 (2010); doi: 10.1063/1.3478465
View online: http://dx.doi.org/10.1063/1.3478465
View Table of Contents: http://scitation.aip.org/content/aip/journal/apl/97/6?ver=pdfcov
Published by the AIP Publishing

Mie scattering enhanced near-infrared light response of thin-film silicon solar cells

S. Nunomura,[a] A. Minowa, H. Sai, and M. Kondo
Research Center for Photovoltaics, National Institute of Advanced Industrial Science and Technology, 1-1-1 Umezono, Tsukuba, Ibaraki 305-8568, Japan

(Received 2 April 2010; accepted 21 July 2010; published online 10 August 2010)

Light trapping is of importance in thin-film silicon solar cells for achieving a higher photocurrent. In this letter, we propose a unique cell structure incorporating submicron-sized light scatterers to enhance light trapping in the near-infrared (NIR) region. The effect of NIR light trapping is demonstrated in substrate-type hydrogenated amorphous/microcrystalline silicon tandem solar cells. By introducing the light scatterers at the interface between the top and bottom subcells, the NIR response of the solar cell is improved, where Mie scattering plays an essential role in increasing the optical path length of the NIR light. © *2010 American Institute of Physics*. [doi:10.1063/1.3478465]

In a thin-film silicon tandem solar cell consisting of hydrogenated amorphous (a-Si:H) and microcrystalline (μc-Si:H) silicon, the a-Si:H top cell absorbs visible light while the μc-Si:H bottom cell absorbs near infrared (NIR) light.[1] Although the μc-Si:H bottom cell requires a thick absorber layer of $\gtrsim 10^2$ μm to sufficiently absorb the NIR light for one single pass,[2] the thickness is limited to $\lesssim 3$ μm in terms of the low-cost approach and carrier transport. For the a-Si:H top cell, the thickness of the absorber layer is limited to $\lesssim 300$ nm because of carrier collection issues. The thinner a-Si:H absorber layer is also preferred for less-pronouncing the light induced degradation.[3] Light trapping is thus required to increase the optical path length of the incident light.

The light trapping is usually achieved by scattering of the incident light at textured interfaces and subsequent internal reflection within the cell.[2] The front transparent conductive oxide/Si and the back reflector/Si interfaces are often textured.[4–6] The ideal shape and feature size of the texture are not fully understood; nevertheless, V- or U-shaped textures with a root mean square roughness of a few tens to a few hundreds of nanometer are used.

In tandem configuration, an intermediate reflector layer (IRL) can be integrated between the top and bottom cells for light management.[7–10] The roles of IRL are reflection of the visible light back into the top cell and transmission of the incoming NIR light to the bottom cell. By incorporating the IRL, the spectra responses of both the subcells are adjusted for the current matching, where both the subcell currents are equalized for obtaining a higher conversion efficiency. Although the visible light response of the top cell is improved with the IRL, a fraction of the NIR light response of the bottom cell is often sacrificed.[10] As an advanced IRL, introducing metallic nanoparticles is proposed for efficient visible light reflection.[11,12]

Here, we propose an another approach to light management, intended to improve the NIR response of solar cells. We consider a tandem cell consisted of two subcells between which submicron-sized light scatterers are placed. A schematic diagram of such an internal light scattering (ILS) solar cell is shown in Fig. 1(a). The interface between the two subcells is chosen for the insertion position of the light scatterers, by taking into account the carrier transport and recombination in tandem operation. The optical properties required for these scatterers are nearly zero absorption and a lower reflective index.

In the ILS cell, Mie scattering[13] plays an essential role in increasing the optical path length. Figure 2 shows the scattering diagrams of the light intensity normalized by a peak value. The diagrams are calculated for the NIR light at a wavelength of $\lambda = 800$ nm scattered from spherical silica particles with the radius of $r_p = 10$, 130, and 500 nm embedded in the medium of Si.[14] The refractive indexes, $n_2 = 1.45$ for silica and $n_1 = 3.7 + i0.007$ for Si, are assumed.[15] As shown, the forward scattering is more pronounced for a larger particle. This forward scattering is a key to increase the optical path length (denoted by the ray 1 in Fig. 1) and induces the subsequent internal reflection (the ray 2).

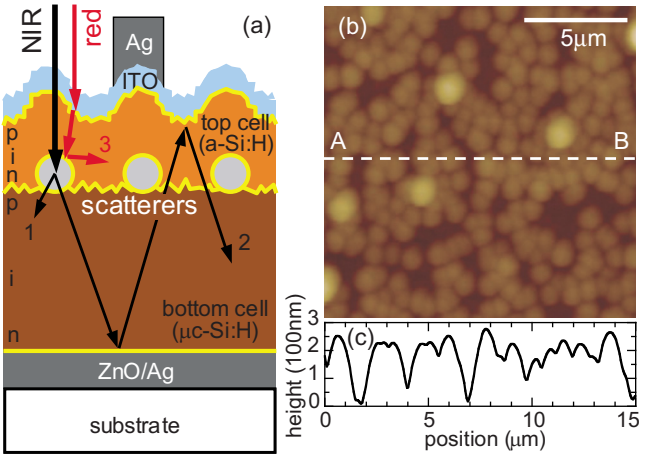

FIG. 1. (Color online) (a) Schematic diagram of the ILS solar cell. The submicron light scatterers are placed at the interface between the top and bottom cells. The incident NIR light is scattered in the forward direction from the scatterers (ray 1), and trapped by the subsequent internal reflection (ray 2), which result in the enhanced NIR response of the bottom cell. The incident red light is reflected by the scatterers (ray 3), yielding the red response improvement of the top cell. (b) AFM image of the surface of the ILS cell. Bright spots correspond to the positions of silica particles embedded in the ILS cell. Brighter and larger spots reflect coagulated particles. (c) Surface profile over a A-B dashed line in Fig. 1(b).

[a]Electronic mail: s.nunomura@aist.go.jp.

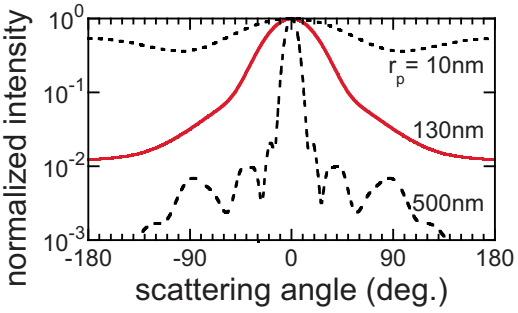

FIG. 2. (Color online) Scattering diagrams of the NIR light intensity at $\lambda=800$ nm. The diagrams are calculated for spherical silica particles with $r_p=10$, 130, and 500 nm in the medium of Si. For comparison, the intensity is normalized by the peak value at a scattering angle of 0°.

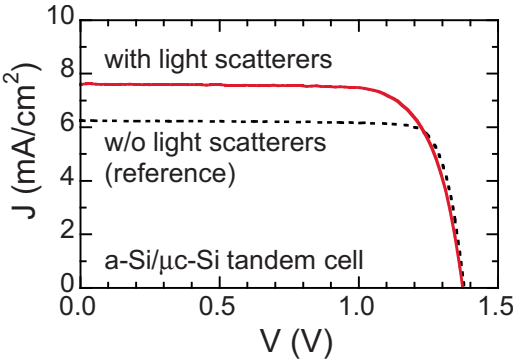

FIG. 4. (Color online) $J-V$ characteristics of the ILS and reference cells ($t_{bottom}=1.0$ μm) under 1 sun illumination.

The NIR light can be efficiently scattered from submicron silica particles embedded in Si. Figure 3 shows the scattering cross sections, $\sigma/\pi r_p^2$, versus r_p. The cross section increases proportionally to r_p^4 at a size parameter of $x=2\pi r_p n_1/\lambda \ll 1$ (Rayleigh regime), and then saturates at $x \gtrsim 1$ (Mie regime) with small oscillations.

We fabricated substrate-type *n-i-p* a-Si:H/μc-Si:H double junction tandem solar cells on flat glass substrates. The solar cell consisted of Ag back contact (200 nm)/Ga-doped ZnO (GZO, 35 nm)/*n-i-p*(μc-Si:H) layers/light scatterers/*n*(μc-Si:H)-*i*(a-Si:H)-*p*(μc-Si:H) layers/Sn-doped In_2O_3(ITO, 75 nm)/Ag front contact. The cell size was 5 mm$\times$5 mm and the active area was 0.215 cm^2. The μc-Si:H *n-i-p* layers and a-Si:H *i*-layer were deposited by plasma enhanced chemical vapor deposition. The back and front contact, GZO and ITO layers were deposited by magnetron spattering. The *i*-layer thicknesses of a-Si:H top and μc-Si:H bottom cell were 350 nm and $t_{bottom}=0.5-1.6$ μm, respectively. Such thin bottom cell absorbers are intended to clearly show the current gain by the NIR light trapping.

The light scatterers were incorporated in the ILS solar cell as follows. Firstly, the μc-Si:H bottom cell was prepared, and the scatterers were dispersed by spin-coating over that. Then, the a-Si:H top cell was deposited on top of that. In this study, spherical silica particles with a size dispersion of $r_p=130\pm13$ nm were used as the scatterers. Micron-sized large particles were not used because they caused a coverage problem of the a-Si:H top cell, inducing current leakage or shunt. During the spin coating, the particles were dispersed as a monolayer, in which the particles were randomly distributed, as shown by an atomic force microscope (AFM) image in Fig. 1(b). The number density of the particles was $n_s \approx 0.98$ μm^{-2} and the corresponding mean interparticle distance was $2a=2/(\pi n_s)^{1/2} \approx 1.1$ μm. The number density was controlled by the concentration of a colloidal solution (silica particles diluted with an ethanol solvent).

By incorporating the light scatterers in a solar cell, the photocurrent was significantly increased. Figure 4 shows the current density versus voltage ($J-V$) characteristics of the ILS and reference cells ($t_{bottom}=1.0$ μm) under 1 sun illumination (air mass 1.5 and 100 mW/cm^2). The reference cell denotes a cell without the scatterers. The short circuit current increases from $J_{sc}=6.3$ mA/cm^2 for the reference cell to 7.3 mA/cm^2 for the ILS cell, by 16%. The current gain gives a rise of the conversion efficiency from $\eta=7.2\%$ to 7.9% whereas the fill factor (FF) reduces from 0.84 to 0.76. This reduction in FF is due to the insertion of the silica particles that induces an increase in the series resistance. The open circuit voltage remains almost unchanged, $V_{oc}=1.38$ V. Both the ILS and reference cells were of the same batch to eliminate interbatch variability.

The observed photocurrent increase is attributed to an improved NIR response of the bottom cell. The quantum efficiency spectra for both the top and bottom cells, QE_{top} and QE_{bottom}, are shown in Fig. 5. Comparing the QE_{bottom} spectra in the NIR region, QE_{bottom} for the ILS cell is higher than that for the reference cell. Correspondingly, the bottom cell current is increased from $J_{bottom}=6.3$ mA/cm^2 to 7.3 mA/cm^2. The subcell currents are computed from J_i

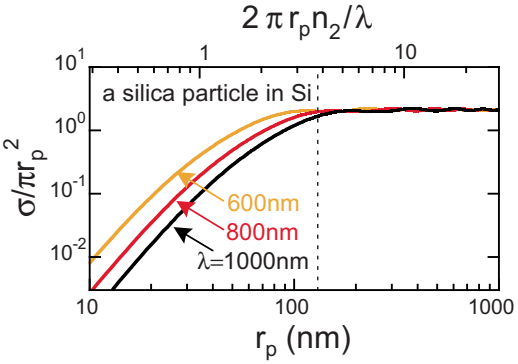

FIG. 3. (Color online) Scattering cross sections of the incident light at $\lambda=600$, 800, and 1000 nm. The cross sections are calculated for a spherical silica particle in the medium of Si. The size of light scatterers used in the ILS cell is shown by a dashed line.

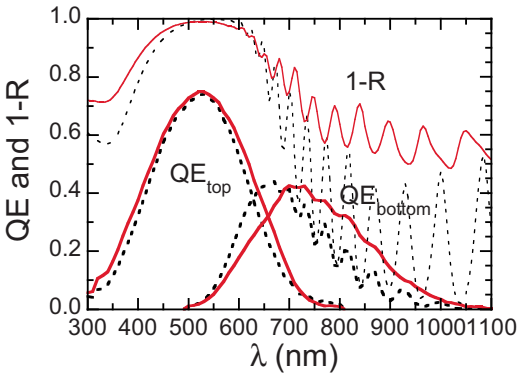

FIG. 5. (Color online) QE and 1-*R* spectra. The spectra for the ILS and reference cells ($t_{bottom}=1.0$ μm) are shown by solid and dotted curves, respectively. The NIR response of the ILS cell is higher than that of the reference cell.

TABLE I. Subcell currents of the ILS and reference cells. Ref. denotes a cell without light scatterers.

Cell type	Substrate	t_{bottom} (μm)	J_{top} (mA/cm^2)	J_{bottom} (mA/cm^2)
ILS (ref.)	Flat	0.5	11.2 (10.5)	4.5 (3.8)
ILS (ref.)	Flat	1.0	11.0 (10.1)	7.3 (6.3)
ILS (ref.)	Flat	1.6	11.1 (10.6)	9.7 (9.2)
Ref.	Texture	1.6	(10.0)	(10.2)

$=e\int \mathrm{QE_i}(\lambda)F(\lambda)d\lambda$, where e and $F(\lambda)$ are the elementary charge and the solar spectrum (air mass 1.5).

Such an improved NIR response results from the NIR light scattering and subsequent internal light trapping, which are confirmed by reflection spectra of the solar cells. As shown in Fig. 5, the reflectivity, R, exhibits distinctive interference fringes in the NIR region formed by the superposition of coherent waves of light reflected at the front and back contacts. This interference fringes are less-pronounced for the ILS cell, indicating an evidence of superposition of incoherent waves, i.e., the light scattering. Also, a reduction in R over the NIR region suggests an increase in the absorption of the NIR light at the bottom cell.

Interestingly, the red light response of the top cell was improved in the ILS cell. The $\mathrm{QE_{top}}$ spectrum in Fig. 5 shows the red light response is slightly extended to longer λ. This enhanced red light response can be interpreted by Fresnel reflection of the red light from the scatterers, i.e., the same effect as the IRL, as indicated by ray 3 in Fig. 1(a). The corresponding top cell current increases from $J_{top}=10.1$ mA/cm^2 to 11.0 mA/cm^2.

The current gains in both the subcells were confirmed for the ILS cells with different t_{bottom}, as listed in Table I. Incorporating the light scatterers at $n_s \sim 0.5-1.0$ μm^{-2} leads to a current gain by $\gtrsim 0.5$ mA/cm^2 for both the subcells. We also checked that a ILS cell ($t_{bottom}=1.6$ μm) yielded nearly equivalent subcell currents of a conventional cell fabricated on a textured substrate (Asahi U-type), as listed in Table I.

In the ILS cells, the cell surface was roughened by incorporating the light scatterers, as shown in Fig. 1(c). The roughness of the cell surface usually leads to light trapping as described in the introduction,[16] and thus improvements of both the NIR and red light response of the ILS cells are enhanced by this effect.

To conclude, we proposed the ILS solar cell to improve the NIR light response. The photocurrent increases were demonstrated in substrate-type a-Si:H/μc-Si:H tandem cells, in which Mie scattering played a role in increasing the optical path length. The ILS solar cell has an beneficial effect of the spectral redistribution to each subcell.

We acknowledge T. Matsui for fruitful discussions. This work was supported by the New Energy and Industrial Technology Development Organization (NEDO).

[1] J. Meier, P. Torres, R. Platz, S. Dubail, U. Kroll, J. A. A. Selvan, N. Pellaton-Vaucher, C. Hof, D. Fischer, H. Keppner, A. Shah, K.-D. Ufert, P. Giannoules, and J. Koehler, *Amorphous Silicon Technology*, MRS Symposia Proceedings No. 420 (Materials Research Society, Pittsburgh, 1996), p. 3.
[2] J. Muller, B. Rech, J. Springer, and M. Vanecek, Sol. Energy **77**, 917 (2004).
[3] D. Staebler and C. Wronski, Appl. Phys. Lett. **31**, 292 (1977).
[4] M. Berginski, J. Hupkes, M. Schulte, G. Schope, H. Steibig, B. Rech, and M. Wuttig, J. Appl. Phys. **101**, 074903 (2007).
[5] T. Söderström, F.-J. Huag, V. Terrazzoni-Daudrix, and C. Ballif, J. Appl. Phys. **103**, 114509 (2008).
[6] H. Sai and M. Kondo, J. Appl. Phys. **105**, 094511 (2009).
[7] K. Yamamoto, A. Nakajima, M. Yoshimi, T. Sawada, S. Fukuda, T. Suezaki, M. Ichikawa, Y. Koi, M. Goto, and T. Meguro, Prog. Photovoltaics **13**, 489 (2005).
[8] P. Buehlmann, J. Bailat, D. Domine, A. Billet, F. Meillaud, A. Feltrin, and C. Ballif, Appl. Phys. Lett. **91**, 143505 (2007).
[9] A. Bielawny, J. Upping, P. T. Miclea, R. B. Wehrspohn, C. Rockstuhl, F. Lederer, M. Peters, L. Steidl, R. Zentel, S.-M. Lee, M. Knez, A. Lambertz, and R. Carius, Phys. Status Solidi A **205**, 2796 (2008).
[10] T. Söderström, F.-J. Haug, X. Niquille, V. Terrazzoni, and C. Ballif, Appl. Phys. Lett. **94**, 063501 (2009).
[11] S. Fahr, C. Rockstuhl, and F. Lederer, Appl. Phys. Lett. **95**, 121105 (2009).
[12] E. Moulin, P. Luo, B. Pieters, J. Sukmanowski, J. Kirchhoff, W. Reetz, T. Muller, R. Carius, F. X. Royer, and H. Stiebig, Appl. Phys. Lett. **95**, 033505 (2009).
[13] H. C. van de Hulst, *Light Scattering by Small Particles* (Dover, New York, 1981).
[14] SCATLAB Version 1.2.0.111, V. Bazhan (http://www.scatlab.com/index.html).
[15] E. D. Palik, *Handbook of Optical Constants of Solids* (Academic, New York, 1985).
[16] H. Sai, H. Jia, and M. Kondo, "Impact of front and rear texture of thin-film microcrystalline silicon solar cells on their light trapping properties," J. Appl. Phys. (in press).